Chidamide inhibits the NOTCH1-MYC signaling axis in T-cell acute lymphoblastic leukemia

Mengping Xi, Shanshan Guo, Caicike Bayin, Lijun Peng, Florent Chuffart, Ekaterina Bourova-Flin, Sophie Rousseaux, Saadi Khochbin, Jian-Qing Mi, Jin Wang

Chidamide inhibits the NOTCH1-MYC signaling axis in T-cell acute lymphoblastic leukemia

Mengping Xi, Shanshan Guo, Caicike Bayin, Lijun Peng, Florent Chuffart, Ekaterina Bourova-Flin, Sophie Rousseaux, Saadi Khochbin, Jian-Qing Mi, Jin Wang

Chidamide inhibits the NOTCH1-MYC signaling axis in T-cell acute lymphoblastic leukemia

Mengping Xi[1,2,*], Shanshan Guo[1,2,*], Caicike Bayin[1,2,*], Lijun peng[1,2], Florent Chuffart[2,3], Ekaterina Bourova-Flin[2,3], Sophie Rousseaux (✉)[2,3,#], Saadi Khochbin (✉)[2,3,#], Jian-Qing Mi (✉)[1,2,#], Jin Wang (✉)[1,2,#]

[1]*Shanghai Institute of Hematology, State Key Laboratory of Medical Genomics, National Research Center for Translational Medicine at Shanghai, Ruijin Hospital Affiliated to Shanghai Jiao Tong University School of Medicine, Shanghai 200025, China;* [2]*Pôle de Recherches Sino-Français en Science du Vivant et Génomique, Shanghai 200025, China;* [3]*CNRS UMR 5309/INSERM U1209/Université Grenoble Alpes/ Institute for Advanced Biosciences, 38706 La Tronche, France*

Abstract **T-cell acute lymphoblastic leukemia (T-ALL) is one of the most dangerous hematological malignancies, with high tumor heterogeneity and poor prognosis. More than 60% of T-ALL patients carry *NOTCH1* gene mutations, leading to abnormal expression of downstream target genes and aberrant activation of various signaling pathways. We found that chidamide, an HDAC inhibitor, exerts an antitumor effect on T-ALL cell lines and primary cells including an anti-NOTCH1 activity. In particular, chidamide inhibits the NOTCH1-MYC signaling axis by down-regulating the level of the intracellular form of NOTCH1 (NICD1) as well as MYC, partly through their ubiquitination and degradation by the proteasome pathway. We also report here the preliminary results of our clinical trial supporting that a treatment by chidamide reduces minimal residual disease (MRD) in patients and is well tolerated. Our results highlight the effectiveness and safety of chidamide in the treatment of T-ALL patients, including those with *NOTCH1* mutations and open the way to a new therapeutic strategy for these patients.**

Keywords T-cell acute lymphoblastic leukemia; HDAC inhibitor; chidamide; NOTCH1; MYC; ubiquitination

Introduction

T-cell acute lymphoblastic leukemia (T-ALL) is a hematological malignant tumor characterized by clonal proliferation of primitive and naive lymphoblasts in the bone marrow, accounting for about 25% of adult ALL [1–3]. Adult T-ALL has poor sensitivity to chemotherapy and the long-term survival rate is less than 50% [4,5]. About half of T-ALL patients suffer recurrence within one year, and the prognosis for relapsed patients is poor [6,7]. Therefore, adult T-ALL patients are in urgent need of new treatment strategies.

Received March 11, 2021; accepted June 25, 2021

Correspondence: Jin Wang, jinwang@shsmu.edu.cn;
Jian-Qing Mi, jianqingmi@shsmu.edu.cn;
Saadi Khochbin,
saadi.khochbin@univ-grenoble-alpes.fr;
Sophie Rousseaux,
sophie.rousseaux@univ-grenoble-alpes.fr

*,# Contributed equally to the work.

The malignant transformation of T cells is a multi-step process, which is maintained by the activation of strong oncogenic drivers that affect cell metabolism and cell cycle [8,9]. More than 60% of T-ALL patients carry oncogenic mutations in the *NOTCH1* [10,11]. In addition, about 20% of patients with T-ALL carry *FBWX7* mutation [12,13], extending the half-life of the active intracellular form of NOTCH1 (NICD1). These two convergent mechanisms lead to the abnormal activation of NOTCH signaling in T-ALL, which becomes the main oncogenic regulator of leukemia cell growth and metabolism [14,15]. The γ-secretase inhibitors (GSIs) can effectively inhibit NOTCH signaling by blocking NOTCH1 intramembrane proteolytic processing through the inhibition of the γ-secretase complex. However, the low clinical response rate of T-ALL to GSIs, combined with severe side effects and high drug resistance rates, are important clinical limitations of this treatment [16]. Additionally, GSIs do not show any specific effect on T-ALL tumors harboring *NOTCH1* mutations [17]. Therefore, it is of critical importance to identify direct *NOTCH1* target genes with oncogenic function.

As a target gene of *NOTCH1* [18,19], *MYC* (also termed c-MYC) [20] has been confirmed to be the central oncogene in T-ALL [21]. Indeed, the oncogenic activity of NOTCH1 in T-ALL is strictly dependent on the upregulation of MYC, which makes MYC a very attractive therapeutic target for the treatment of T-ALL [22,23]. However, MYC lacks specific active sites for small molecule inhibitors, which has been an important obstacle for direct targeting of MYC for decades [24].

Based on this observation, we sought a research strategy aiming at an effective suppression of the NOTCH1-MYC control loop.

Histone deacetylase (HDAC) inhibitors can cause the downregulation of MYC expression in a variety of blood tumor types, and can reactivate aberrantly repressed tumor-suppressor genes to exert a strong anti-tumor effect [25,26]. Moreover, it has previously been shown that the non-selective HDAC inhibitor (HDACi), panobinostat, exerts its pro-apoptotic and anti-proliferative effects by inhibiting *NOTCH1* target gene expression in T-ALL [27]. Among HDACi target enzymes, HDAC3 directly controls the stability of NOTCH1 by regulating its acetylation level [28]. Additionally, by inducing histone hyperacetylation, HDACi could also modulate general oncogenic transcriptional activity, specifically those dependent of bromodomain-containing factor BRD4 [29,30]. Therefore, through acting at different levels, transcriptional and post-transcriptional, HDAC inhibitors constitute potential therapeutic strategies for targeting oncogenic gene expression programs including the NOTCH1-MYC signaling axis.

Chidamide is a new type of selective HDAC inhibitor that specifically inhibits class 1 enzymes: HDAC1, HDAC2, HDAC3 as well as HDAC10 [31]. *In vitro* and in mouse models of various hematological malignancies, chidamide has demonstrated robust anti-tumor activities including pro-apoptotic and anti-proliferative effects [32–36]. Additionally, in previously published clinical trials, chidamide also showed little toxic side effects and was well tolerated [37,38]. Remarkably, in refractory or relapsed T-LBL/ALL patients, chidamide-treated patients also had a better progress-free survival (PFS) compared to patients of the chemotherapy group [39].

Despite these encouraging clinical data, there is no report on the mechanism of action of chidamide in T-ALL. Accordingly, we elaborated a research project to investigate the molecular basis of chidamide action in T-ALL, laying a solid foundation for the subsequent further clinical research.

Materials and methods

Reagents and antibodies

DMSO was purchased from Sigma-Aldrich (St. Louis, MO, USA). Chidamide was provided from the Chipscreen Company (Shenzhen, Guangzhou, China), dissolved in DMSO at a 100 mmol/L concentration. Fetal bovine serum was purchased from Sigma-Aldrich (St. Louis, MO, USA). MYC, cyclin D1, anti-histone H3, anti-histone H3 (acetyl K27) antibodies were purchased from Abcam (Cambridge, MA, USA); β-actin antibody was bought from Sigma-Aldrich; caspase-9, caspase-8, caspase-3, cleaved-caspase-3, PARP, cleaved PARP, Bcl-2, Bcl-xL, Bid, p21, mouse anti-rabbit IgG and NICD1 antibodies were purchased from Cell Signaling Technology (CST, Danvers, MA, USA). CHX was purchased from Sigma, and MG132 was bought from Selleck (Shanghai, China).

Cell culture

Acute lymphoblastic leukemia cell lines, including Jurkat and MOLT-4, were both incubated in RPMI 1640 (Gibco, Billings, MT, USA) supplemented with 10% fetal bovine serum (Gibco, USA) at 37 °C in a 5% CO_2 atmosphere. The T-ALL patients' primary cells involved in the experiment were isolated from the patients' bone marrow and incubated in IMDM (Gibco) containing 20% fetal bovine serum (Gibco).

Patient characteristics and treatment regimen of clinical trial (ChiCTR-ONRC-14004968)

Patients in our center newly diagnosed with T-ALL or suffering from relapse by histology or cytology after 2017, were enrolled in the study according to the following criteria: primary refractory status after induction therapy, or relapse after first complete remission (CR), and Eastern Cooperative Oncology Group (ECOG) score $\leqslant 2$. Patients were excluded if they had severe heart, kidney, liver, or major organ dysfunction. The patient's clinical information is described in detail in Dataset S1. The treatment regimen included chidamide (10 mg qd day –2 to day 10) combined with Hyper-CVAD-A (cyclophosphamide, vincristine, doxorubicin, and dexamethasone), alternating with chidamide (10 mg qd day –2 to day 10) combined with Hyper-CVAD-B (alternate use of high-dose methotrexate and cytarabine) monthly.

Human samples

Peripheral blood or bone marrow samples from T-ALL patients were collected from Ruijin Hospital (Shanghai, China). According to the *Declaration of Helsinki*, all patients or their families involved in this study obtained informed consent, all T-ALL patients involved in the experiment have signed an informed consent. The research content was approved by the review committee of Ruijin Hospital and relevant scientific research institutions.

Separation of the patients' lymphocytes

Each patient's bone marrow was diluted with equal volume of PBS solution. Lymphocyte separation fluid (Lymphoprep™ 07801, Stemcell, USA) was added to the centrifuge tube, and the diluted mixture was spread over the separation liquid and centrifuged at 2800 rpm for 25 min at room temperature (RT). The mononuclear cells (including lymphocytes and monocytes), between the plasma layer and the separation fluid, were collected.

MRD assessment by multiparameter flow cytometry (MFC)

Minimal residual disease (MRD) is the most important factor in the prognostic stratification of acute lymphoblastic leukemia (ALL). At present, our Clinical Laboratory Center has been using 8-10 color flow cytometry to monitor the leukemia-related immunophenotype of ALL patients [40]. At the time of the patient's initial diagnosis, leukemia-associated immunophenotype (LAIP) was determined by flow cytometry, and the leukemia cells were monitored using LAIP as a benchmark. When the residual leukemia cells in the bone marrow of the patient after treatment are less than 0.01%, the MRD is considered negative. Depending on the treatment stage of the patient, the time points for obtaining bone marrow are different: MRD was detected on day 14 and day 28 during induction phase; MRD was monitored regularly during consolidation and maintenance phase.

The detailed detection method is as follows. Fresh heparinized whole bone marrow (BM) samples are processed according to the standard NH_4Cl whole blood lysis technique for immunophenotyping and MRD is monitored. In short, BM samples containing up to 3×10^6 WBCs were incubated with the titrated reagent mixture, then incubated in the dark at RT for 15 min, and then incubated in 2.0 mL of NH_4Cl containing 0.25% ultrapure formaldehyde (Polysciences, Warrington, PA, USA), incubated in the dark at RT for 15 min, then washed once with 0.3% bovine serum albumin-containing phosphate buffered saline. When 200 μL BM was not sufficient to collect at least 3×10^6, before the staining process, a lysis procedure of WBCs was performed, followed by a single wash. Fix-and-Perm kit was used to process the BM for evaluation of TdT and cytoplasm (Cy) CD79a and IgM (cμ). Dead cells and debris were excluded by forward scatter (FSC)/SSC and CD45/SSC dot plots. Double peaks were not included in the FSC-A/FSC-H dot plots. For LAIP, the FACSDiva software (Becton Dickinson, San Jose, CA, USA) was used to define the final MRD group.

NOTCH1 mutation detection in patients

Total RNA was extracted using TRIzol agent (Invitrogen, Carlsbad, CA, USA). First-strand cDNA was synthesized from 1 μg total RNA using Superscript II reverse transcriptase (Invitrogen) and random hexamers according to the instructions of the manufacturer. The transmembrane segment and intracellular region of NOTCH1 were amplified using standard protocol with seven pairs of primers as previously described [41]. The resultant PCR products were purified on Qiagen columns (Qiagen, Inc., Valencia, CA, USA) and sequenced by NOTCH1 primers on ABI Prism 3700 DNA Analyzer using BigDye Terminator v3.1 Cycle Sequencing Kit (Applied Biosystems, Foster City, CA, USA).

Cell viability assay

2.5×10^5/mL Jurkat cells and 3×10^5/mL MOLT-4 cells were calculated in 96-well plates (each well contained 100 μL of cell suspension). After treatment with chidamide for 24, 48 or 72 h, 10 μL of CCK8 (Dojindo Laboratories, Kumamoto, Japan) was added to each well and incubated for another 1.5 h at 37 °C in a 5% CO_2 atmosphere. Absorbance of the samples was measured against a background control at 450 nm. Cell viability was calculated using the following equation: proliferation (%) = (OD450 of isogarcinol group/OD450 of control group) × 100%.

Cell apoptosis assay

2×10^5 cells were collected and washed with 1 × PBS and re-suspended in 200 μL binding buffer with 5 μL of annexin V–FITC and 5 μL propidium iodide (PI) (BD Pharmingen, San Diego, CA, USA). Flow cytometry was performed to analyze 1×10^5 cells. The stained cells were analyzed on the LSR Fortessa TM X-20 flow cytometer (Becton Dickinson, San Diego, CA, USA). All data were analyzed by FlowJo Vision10 (TreeStar).

Cell cycle assay

2×10^6 cells were washed with cold 1 × PBS and centrifuged at 4 °C for 5 min at 400× *g* twice, mixed with cold 70% ethanol, then fixed at 4 °C overnight. The stained cells were collected by centrifugation, washed once with 1 mL of PBS, then the cells were re-suspended in PBS supplemented with 100 μg/mL DNase-free RNase A (QIAGEN) and 100 μg/mL PI (Sigma) incubated for another 15 minutes. Samples were analyzed on the LSR Fortessa TM X-20 flow cytometer (BD Biosciences, USA). All data were analyzed by ModFit software (ModFit LT 3.1).

HDAC activity analysis

DMSO and chidamide (2 μmol/L) were added to the Jurkat

and MOLT-4 cells and incubated at 37 °C for 48 h. HDAC activity was detected as described in the Colorimetric HDAC Activity Assay kit (BioVision, San Francisco, USA). Every reaction included the nuclear protein (100 μg) extracted from Jurkat and MOLT-4 cells, 10 μL HDAC assay buffer and 5 μL HDAC colorimetric substrate. Plates were incubated at 37 °C for 1 h and the reaction was stopped by adding 10 μL of lysine developer and plates incubated at 37 °C for 30 min. Absorbance of the samples was measured at 405 nm. HDAC activity can be expressed as the relative OD value per μg protein sample.

RNA isolation and real-time polymerase chain reaction (RT-PCR)

Total cellular RNA was extracted from 1×10^7 cells using Trizol reagent (Invitrogen, Carlsbad, CA, USA) according to the manufacturer's protocols. RNA was eluted with RNase-free water, quantified at an absorbance at 260/280 nm and used for reverse transcription reaction. The mRNA was reversely transcribed into cDNA using HieffTM First Strand cDNA Synthesis Kit (YEASEN, Shanghai, China). Real-time PCR assay was performed using HieffTM qPCR SYBR Green Master Mix (Low Rox Plus) (YEASEN, Shanghai, China). The primers were as follows: NOTCH1 (Forward: ACTGTGAGGACCTGGTGGAC; Reverse: TTGTAGGTGTTGGGGAGGTC); MYC (Forward: TACCCTCTCAACGACAGCAG; Reverse: TCTTGACATTCTCCTCGGTG); GAPDH (Forward: GAAGGTGAAGGTCGGAGTC; Reverse: GAAGATGGTGATGGGATTTC). The RT-PCR conditions were as follows: 1 cycle at 95 °C for 30 s, 40 cycles at 95 °C for 10 s, 60 °C for 30 s, and one cycle at 72 °C for 20 s. Amplifications were performed in a 7500 Real-time PCR System (Applied Biosystems, Foster City, CA, USA).The results were analyzed using 2-ΔΔCt, in which ΔCt = Ct (target gene) − Ct (internal reference), ΔΔCt = ΔCt (sample) − ΔCt (control). Each sample was analyzed in triplicates.

Western blot assay

1×10^7 cells were collected and washed twice with precooled 1 × PBS, and centrifuged at 4 °C for 5 min at 800 rpm. Total cell lysates were extracted by protein lysate mixture (RIPA buffer: 1 mmol/L PMSF: 1 × cocktail = 1000:1:0.1). Equal amounts of proteins were separated by 6%–15% SDS-PAGEs and transferred to PVDF membranes. PVDF membranes were incubated overnight at 4 °C with the primary antibodies, after being blocked with 5% BSA for 1 h at RT. After three washes with 1 × TBST, each membrane was incubated with HRP-goat-anti-mouse IgG or anti-rabbit IgG (CST, USA) as secondary antibody for 1 h at 4 °C. The expressions of the proteins were detected by enhanced chemiluminescence kits (Millipore, Billerica, MA, USA).

Cycloheximide (CHX) chase assay

Jurkat and MOLT-4 cells were randomly divided into two groups, one with DMSO and the other with 2 μmol/L chidamide. In the same conditions, the two groups of cells were incubated for 24 h at 37 °C in a 5% CO_2 atmosphere. Subsequently, both groups of cells were given 10 μg/mL of CHX (Sigma, USA) at the same time. Total cell lysates were collected at successively 2 h, 4 h, and 8 h after adding CHX and prepared to Western blot assay.

Immunoprecipitation assay (IP)

3×10^7–4×10^7 cells were collected and centrifuged at 800 rpm at 4 °C for 5 min. Each of the cell pellets was washed twice with cold PBS at 4 °C for 5 min. After 0.7 mL of cell lysis suspension (1 × lysis buffer (Thermo Fisher, USA), 1 × PMSF (Selleck Chemicals, Houston, TX, USA), 1 × NEM (Selleck Chemicals, USA)) was added to the cell pellet and mixed, the samples were treated with ultrasound (10 times 30 s at intervals of 30 s), centrifuged at 12 000 rpm for 5 min, and the supernatant was collected. After adding 5 μg of purified antibody, the cell lysate was incubated overnight at 4 °C, transferred to a spin column and incubated overnight at 4 °C. It was then centrifuged at 3000 rpm for 30 s at 4 °C, and the eluate was saved to detect the binding of the target protein to the antibody. The separation column was washed by centrifugation at 3000 rpm in 1 × PBS at 4 °C then 3 times with 1 × lysis buffer (Thermo Fisher) under the same centrifugal conditions. After addition of 40 μL of 1 × loading buffer, the sample was heated at 95 °C for 5 min, then centrifuged at 12 000 rpm for 30 s. The eluted immunoprecipitates were used for SDS-PAGE. Each membrane was incubated with mouse anti-rabbit IgG (Conformation Specific, CST#5127), a conformation-specific antibody, which only detects IgG with a spatial conformation and does not detect denatured IgG and does not recognize the denatured and reduced rabbit IgG heavy (about 50 kDa) or light (about 25 kDa) chains on Western blot.

RNA sequencing and analysis

1.5×10^7 MOLT-4 or Jurkat cells chidamide-treated (2 μmol/L for 48 h) or untreated cells were collected and washed with 1 × PBS at 400 rpm twice, and 2 mL of Trizol were added to isolate RNA. RNA purity was checked using the Nano Photometer® spectrophotometer (IMPLEN, CA, USA). RNA integrity was assessed using the RNA Nano 6000 Assay Kit of the Bioanalyzer 2100 system (Agilent Technologies, CA, USA). The RNA

library construction and paired end RNA sequencing was performed by Novogene Co., Ltd. (Beijing, China). Sequencing libraries were generated using NEBNext® UltraTM RNA Library Prep Kit for Illumina® (NEB, USA) following manufacturer's recommendations. The clustering of the index-coded samples was performed on a cBot Cluster Generation System using TruSeq PE Cluster Kit v3-cBot-HS (Illumina) according to the manufacturer's instructions. After cluster generation, the library preparations were sequenced on an Illumina Novaseq6000 platform and 150 bp paired-end reads were generated.

The reads were aligned on the hg19 UCSC genome using the ultrafast universal RNAseq aligner STAR [42], the counts were computed into Reads Per Kilobase of transcript, per Million mapped reads (RPKM) using HTseq [43] and normalized with the SARTools (Statistical Analysis of RNA-Seq data Tools) DESeq2-R pipeline [44]. The data of 130 T-ALL patients was deposited in bioinfo.rjh.com.cn/cga (Accession No.CGAS000000-00002) [11]. The data of Jurkat and MOLT-4 cell lines have been deposited on GEO under the ID number (GSE160349).

Statistical analysis

Statistical analysis were performed using GraphPad Prism 8.0 (GraphPad Software Inc., San Diego, CA, USA). All experimental data are expressed as the mean ± S.E.M. Significance was calculated using Student's *t*-test. A two-tailed value of $P < 0.05$ was considered to be significant.

Results

Chidamide induces cell mortality and apoptosis in T-ALL patients' primary cells

To set the basis of our investigations and evaluate cell sensitivity to chidamide, we tested the viability of primary cells extracted from the bone marrow of a series newly diagnosed patients or relapsed patients with T-ALL, with wild-type or mutated *NOTCH1*, after treatment with increasing doses of chidamide during increasing lengths of time. We observed that all the primary cells, irrespective of *NOTCH1* mutation, are sensitive to chidamide treatment. Increasing treatment time reduced the differences in sensitivity of the cells from different patients to chidamide, except for the cells from patient 1 and patient 7, showing a remarkable resistance to chidamide treatment (Fig. 1 and Fig. S6A–S6C).

These investigations using primary cells from T-ALL patients suggested that chidamide is behaving as a general modulator of HDAC signaling and hence could influence a large panel of various oncogenic mechanisms, which could include *NOTCH1* mutation-driven events.

Chidamide treatment induces an arrest of the cell cycle in G0/G1 phase

Our data suggest that cell treatment by chidamide could activate general anti-oncogenic mechanisms. To investigate both NOTCH1-dependent and independent anti-

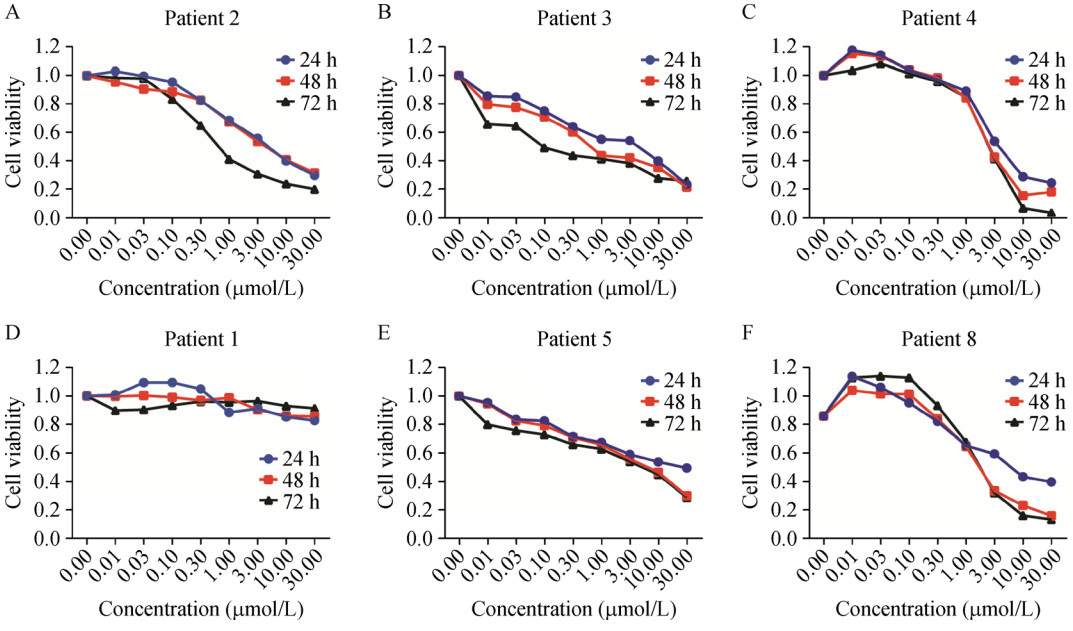

Fig. 1 Chidamide inhibits cell viability in T-ALL patients' primary cells with or without *NOTCH1* mutation. Cell viability after treatment with increasing concentrations of chidamide (as indicated) in primary cells from T-ALL patients with *NOTCH1* mutation (A–C) or without *NOTCH1* mutation (D–F). The three curves respectively in blue, red and black correspond to different durations of treatment of 24, 48, and 72 h.

oncogenic effects of chidamide treatment, we focused our attention on two T-ALL cell lines, Jurkat cells and MOLT-4 cells.

MOLT-4 cells harbor a deletion of a CT dinucleotide in the PEST domain of the *NOTCH1* (heterozygous for c.7541_7542delCT [45]), and a mutation in HD domain of *NOTCH1* (heterozygous mutation 1601 L→P) [46]. Jurkat cells bear an insertion of the 51 bp in exon 28 of *NOTCH1* (c.5220_5221ins51 (CAGGCCGTGGAGCCGCCC-CCGCCGGCGCAGCTGCACTTCATGTACGTGGCG)), resulting in the insertion of 17 amino acids (p.1740_1741insQAVEPPPPAQLHFMYVA) in the extracellular juxtamembrane region of the NOTCH1 receptor [47,48].

We found that, as expected, the treatment of cells with increasing concentrations of chidamide significantly affected cell viability in both cell lines tested (Fig. 2A and Table S1). To make sure that, under our treatment conditions, chidamide is effectively inhibiting its target enzymes, we also measured the global HDAC activity in treated cells and indeed observed a clear decrease in the total cellular deacetylase activity of treated cells from both cell lines compared to that of untreated cells (Fig. 2B). Furthermore, we also tested whether chidamide would also be capable of acting on the classical cell cycle control mechanisms previously reported to be sensitive to HDAC inhibitors [32]. To this end, we compared the distribution of cells in the cell cycle between chidamide-treated and untreated cells. Compared with the non-treated cell group, the proportion of cells in the G0/G1 phase of the chidamide-treated group was significantly increased (Fig. 2C). This is in line with the re-expression of the p21 protein, which is a well-known cell cycle inhibitor protein, induced by various kinds of HDACi [49,50]. p21 is known to inhibit a variety of cyclin-CDK complexes [51]. As expected, we found that the p21 protein level of the two tested cell lines was significantly upregulated, while the cyclin-D1 was significantly downregulated (Fig. 2D). These results demonstrate that chidamide is targeting cell functions that are expected to be targets of a classical HDAC inhibitor, by upregulating p21 and inducing cell cycle arrest in G0/G1 phase. These data show also that in these model cell lines, in addition to its potential role on the specific NOTCH1 pathway, chidamide treatment could also activate the general known HDAC-dependent mechanisms involved in the induction of a cell cycle arrest.

Chidamide induces apoptosis by activating the endogenous apoptotic pathway

We also used our model cell lines to define the pro-apoptotic pathways controlled by chidamide treatment, which could also explain the general NOTCH1-independent anti-oncogenic effects of this treatment. To this end, we treated the cells with different concentrations of chidamide for 24, 48 and 72 h. The results show that, compared with the control group, chidamide can induce an increase in the proportion of apoptosis in the two T-ALL cell lines (Fig. S1). With the increase of drug concentration and treatment time, the apoptosis rate of chidamide-treated group increased significantly (Fig. 3A). To clarify the apoptosis pathway induced by chidamide, we tested the expression levels of caspase family molecules. The results suggest that chidamide induces the cleavage of caspase-3 as it can be judged by a decrease in full-length caspase-3 and the accumulation of its cleaved forms (Fig. 3B). Additionally, a decrease in caspase-9 and accumulation of cleaved-PARP were observed (Fig. 3B). However, no obvious abnormal expression of the caspase-8 molecule was observed, indicating that chidamide induces apoptosis by activating the endogenous apoptosis pathway.

We also observed that in chidamide-treated cells, the expression of Bcl-2 family anti-apoptotic molecules Bcl-2 and Bcl-xL was downregulated, and the expression of pro-apoptotic protein Bim remained almost unchanged (Fig. 3C). These results show that chidamide downregulated the anti-apoptotic molecules Bcl-2 and Bcl-xL, which eventually activated the endogenous apoptotic pathway to induce cell apoptosis.

Chidamide inhibits the NOTCH1-MYC signal axis

So far, we had unraveled several general anti-oncogenic effects of chidamide treatment. However, the question of a specific anti-NOTCH1 effect of chidamide treatment remained open. To better characterize the effect of chidamide on the biology of the two considered cell lines, we obtained RNA-seq data from control and chidamide-treated Jurkat and MOLT-4 cells (see below for more details on RNA-seq experiments). From these RNA-seq data we observed that, upon the treatment of cells with chidamide, the mRNA level of *NOTCH1* was significantly downregulated in the MOLT-4 cell line ($P < 0.05$), whereas no significant change was detected for this gene in the Jurkat cell line ($P = 0.643597$). Under the same conditions, we could not detect any significant change in *MYC* gene expression (Fig. 4A). The RT-qPCR approach confirmed this finding (Fig. 4B and 4C). To show the effect of chidamide treatment at the protein expression levels, we treated the cells with increasing concentrations of chidamide (0.5 μmol/L, 1 μmol/L, and 2 μmol/L). After 48 h of treatment, we found that NOTCH1 and MYC were significantly downregulated in the chidamide-treated cells compared with the untreated control cells (Fig. 4D). Since the protein level is regulated by protein synthesis and protein degradation, ensuring its steady-state concentration, we hypothesized that chidamide may inhibit the NOTCH1-MYC signal axis by promoting the degradation

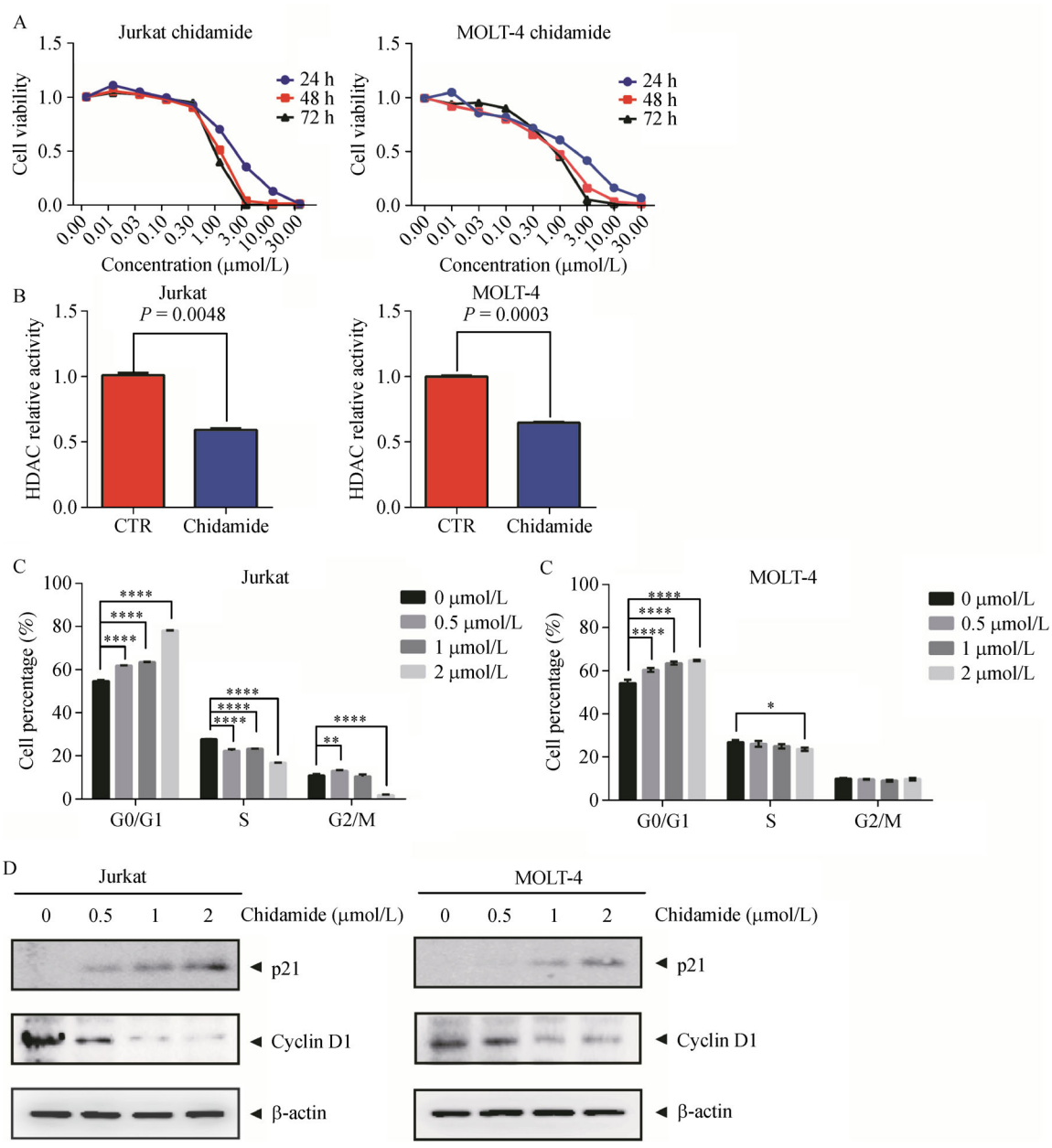

Fig. 2 Chidamide treatment induces an arrest of the cell cycle in G0/G1 phase. (A) In Jurkat and MOLT-4 cell lines cell viability is significantly inhibited by a treatment with chidamide at concentrations above 0.3 to 3 μmol/L. (B) HDAC activity in chidamide-treated cells is significantly reduced compared to untreated cells of both cell lines. HDAC activity in control and chidamide-treated cells were measured by absorbance at 450 nm. (C) The proportion of cells at G0/G1 cell cycle stage is increased after treatment for 48 h with increased concentrations of chidamide (as indicated). * $P < 0.05$, ** $P < 0.01$, **** $P < 0.0001$. (D) p21 increases and cyclin D1 decreases as a function of chidamide concentration in chidamide-treated cells of both Jurkat and MOLT-4 cell lines. Western blot detecting p21 and cyclin D1 in cells treated with different concentrations of chidamide (as indicated) for 48 h.

of NOTCH1 and MYC proteins. Indeed, since at the mRNA level, upon chidamide treatment, the expression of *NOTCH1* decreased only in MOLT-4 cells but was not affected in Jurkat cells and *MYC* mRNA level was not affected either in MOLT-4 or in Jurkat cells, we concluded that in both cell lines chidamide treatment downregulates NOTCH1 and MYC proteins at post-translational levels.

Chidamide promotes the degradation of NICD1 and MYC via the proteasome pathway

To test the hypothesis of a chidamide-controlled post-translational regulation of NOTCH1 (NICD1) and MYC, we first inhibited protein translation by cycloheximide (CHX) for different times in the presence or absence of

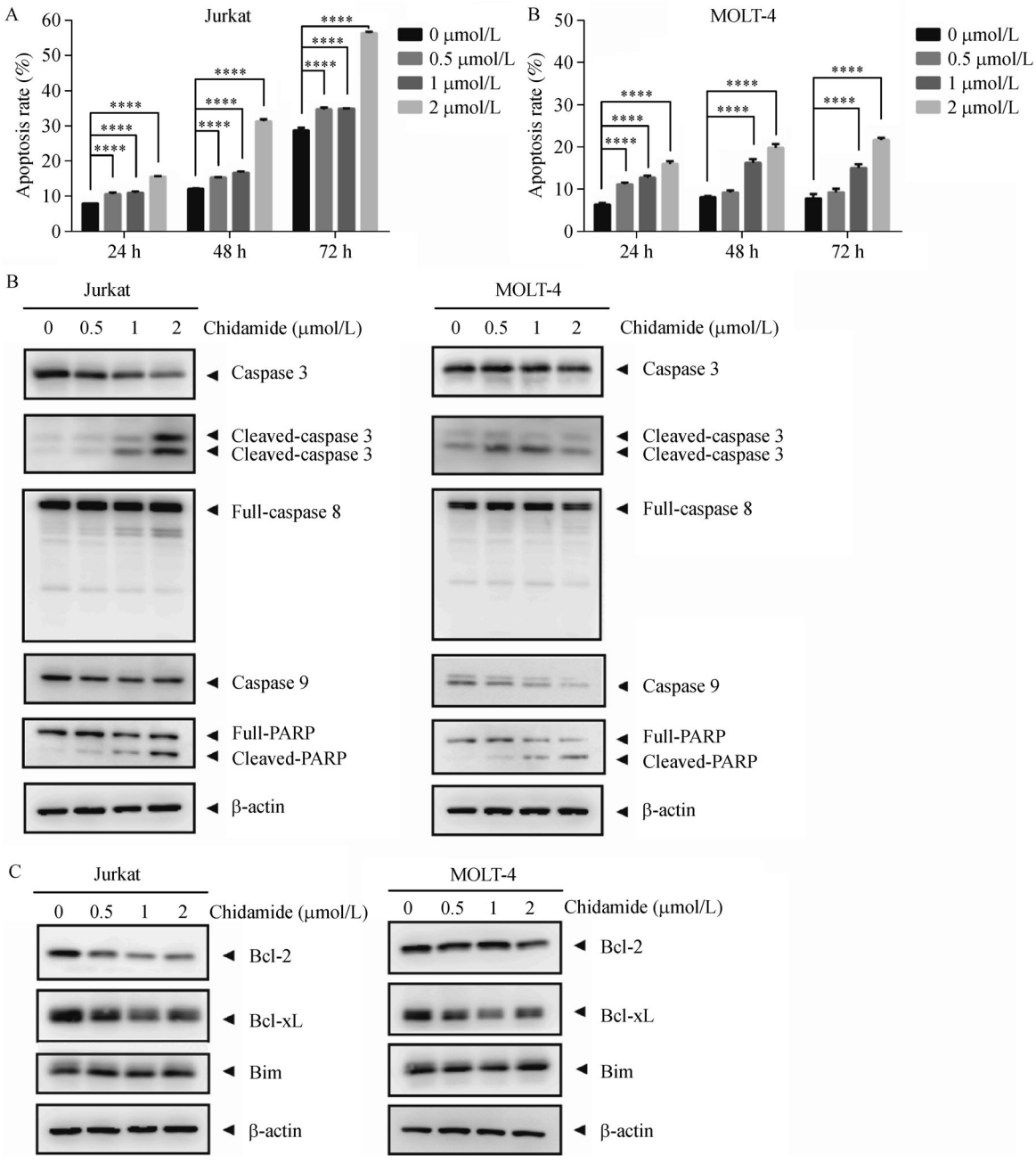

Fig. 3 Chidamide induces apoptosis in NOTCH1 mutant T-ALL cell lines by activating the endogenous apoptotic pathway. (A) Cell apoptosis increases as a function of chidamide concentration and treatment duration. * $P < 0.05$, ** $P < 0.01$, **** $P < 0.0001$. (B) Western blot detecting caspase-3, 8, 9, and PARP in Jurkat and MOLT-4 cells treated with chidamide at the indicated concentrations for 48 h. (C) Western blot detecting anti-apoptotic molecule (Bcl-2 and Bcl-xL) and pro-apoptotic molecule (Bim) in Jurkat and MOLT-4 cells treated with chidamide at the indicated concentrations for 48 h.

chidamide. In both cell lines, MYC was highly unstable and rapidly disappeared after CHX treatment in the presence or absence of chidamide (Fig. 5A and 5B, minus (−) chidamide). Interestingly, NICD1 was relatively more stable in non-treated cells than in treated cells, where chidamide induced a rapid degradation of the protein in both cell lines (Fig. 5A and 5B, plus (+) chidamide). CHX is a protein synthesis inhibitor. When CHX is added to a cell line, protein synthesis can be inhibited, allowing to evaluate the protein degradation rate in presence or absence of chidamide. After 2 h of CHX treatment, in the control cells, NICD and MYC protein levels did not change significantly, whereas in chidamide treated cells the levels of these target proteins were extremely low, hardly

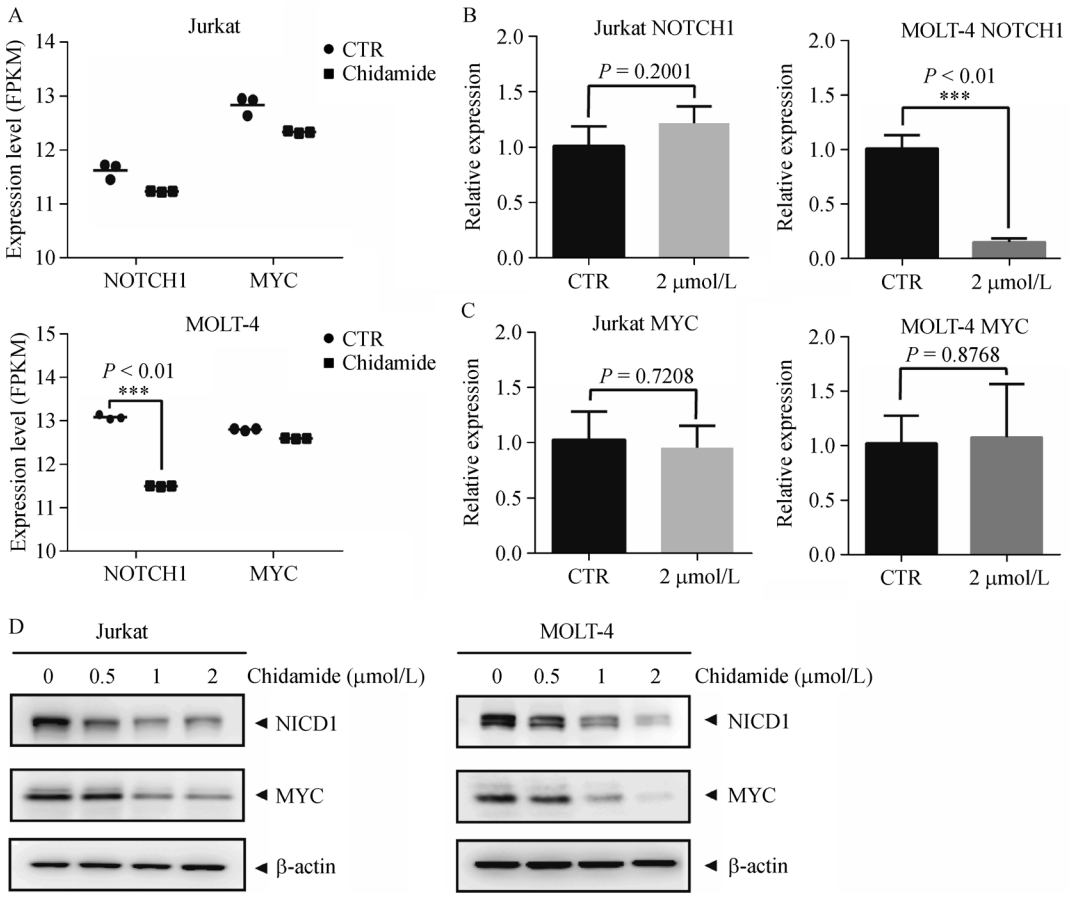

Fig. 4 Chidamide inhibits NOTCH1-MYC signaling axis in both Jurkat and MOLT-4 cell lines by increasing proteasome dependent degradation of both proteins. (A–C) Chidamide does not affect the transcription of NOTCH1 and MYC in Jurkat cells, but inhibits the transcription of NOTCH1 in MOLT-4 cells ($P < 0.01$) as shown in the RNAseq data analysis (A) or RT-QPCR experiments (B and C). (D) Western blot detecting NICD1 and MYC in Jurkat and MOLT-4 cells treated with chidamide at the indicated concentrations for 48 h.

detectable, suggesting that protein degradation was accelerated in chidamide-treated cells compared to control cells.

To clarify the protein degradation pathway controlling the post-translational stability of MYC and NICD1, we treated the cells with MG132, which is a proteasome inhibitor which inhibits protein degradation through the proteasome pathway. We found that the levels of NOTCH1 and MYC in the control group were upregulated after adding MG132, whereas in chidamide-treated cells, the accelerated degradation of NICD1 was abolished by MG132 (Fig. 5C and 5D) demonstrating the MG132 treatment could attenuate the effect of chidamide treatment on protein degradation and confirming a role for chidamide treatment in the control of stability of these two proteins.

To confirm that both NICD1 and MYC are degraded by the proteasome after protein ubiquitination, we immunoprecipitated NICD1 and MYC from the total protein extracts and performed immunodetection assays to detect the ubiquitination levels of both proteins. Compared with the control group, chidamide treatment significantly increased the ubiquitination levels of NICD1 and MYC (Fig. 5E).

Altogether, these data demonstrate that chidamide treatment promotes protein degradation by increasing the ubiquitination levels of NICD1 and MYC, and thereby inhibits the NOTCH1-MYC signal axis.

In summary, our results from patients' primary cells and both Jurkat and MOLT-4 cell lines consistently show that chidamide treatment impacts cell viability and the proliferation of cell lines and patients' primary cells. In cell lines, it acts by upregulating the expression of p21 and inhibiting downstream effector molecules to block the cell cycle at the G0/G1 phase, whereas at the same time it induces apoptosis by activating the endogenous apoptotic pathway.

More specifically, in cells with activated NOTCH oncogenic pathways, chidamide treatment inhibits the NOTCH1-MYC signaling axis by promoting NOTCH1 and MYC degradation.

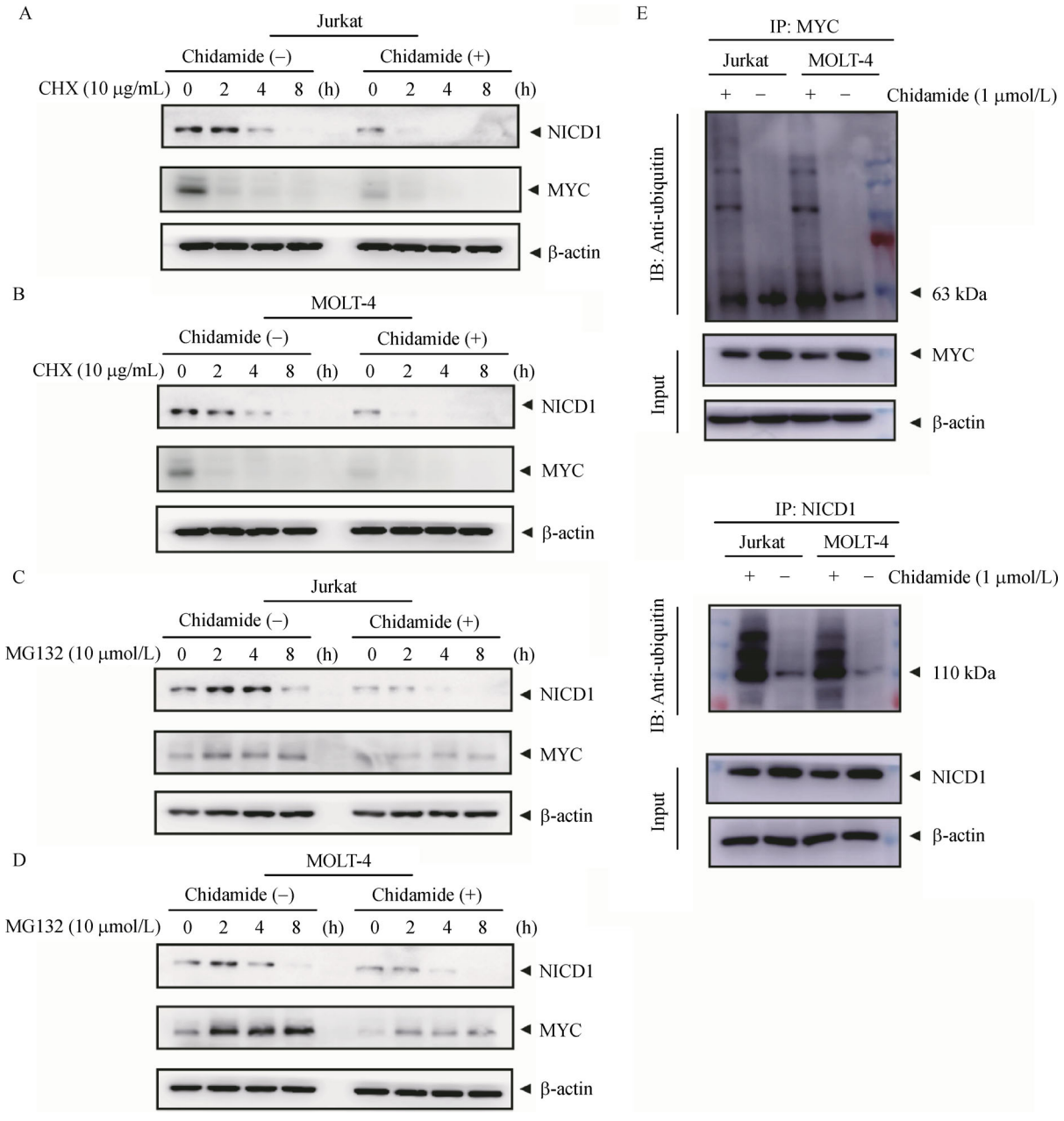

Fig. 5 Chidamide promotes the degradation of NOTCH1 and MYC via the proteasome pathway in both Jurkat (A and C) and MOLT-4 (B and D) cells. (A and B) The chidamide-treated and untreated control cells were cultured under the same culture conditions for 24 h. 10 μg/mL of CHX was added at the same time to chidamide-treated and control cells and Western blots were performed after the indicated periods of time to detect NICD1 and MYC. The degradation rate of NICD1 and MYC proteins in the chidamide-treated cells was faster than that in the untreated control cells. (C and D) The chidamide-treated and untreated control cells were cultured under the same culture conditions for 24 h. 10 μmol/L of MG132 was added at the same time to both chidamide-treated and untreated cells and Western blots were performed after the indicated periods of time to detect NICD1 and MYC. MG132 increased the levels of NICD1 and MYC proteins in both chidamide-treated and untreated cells, suggesting that the two proteins were prevented from being degraded by the proteasome pathway. (E) The proteasome-dependent degradation of both NICD1 and MYC requires their ubiquitination. Immunoprecipitation experiments followed by immunodetection of ubiquitination show that the ubiquitination levels of NICD1 and MYC proteins in the chidamide-treated cells are were significantly increased compared to those in non-treated cells.

Chidamide treatment in *NOTCH1* mutant T-ALL cell lines mediates anti-NOTCH1 effects

To further clarify the mechanisms of chidamide in *NOTCH1* mutant T-ALL cells, we used our two model cell lines, Jurkat and MOLT-4 cells, to perform transcriptomic analyses by RNA sequencing of control and chidamide-treated cells (chidamide 2 μmol/L for 48 h).

For each cell line, we performed an ANOVA to identify differentially expressed genes (Fig. S2A). We found that the gene expression response to chidamide treatment was remarkably correlated between the two tested cell lines with a correlation coefficient of 0.62 between the two signatures (Fig. S2B).

The lists of differentially expressed genes were used to perform KEGG and Gene Ontology (GO) terms enrichment analyses. The KEGG analysis suggested that the differentially expressed genes of the two cell lines are mainly genes known to be expressed in the hematopoietic lineages (Fig. S3A and S3B). In particular, in the GO enrichment analysis of the chidamide response in the Jurkat cell line, we observed that the differentially expressed genes are mostly related to T cell differentiation and activation (Fig. S3C and S3D), which, interestingly, involve processes that are NOTCH1-dependent [52–54].

Geneset enrichment analysis (GSEA) of the chidamide response signature of both cell lines showed that HDAC downstream genes are affected by chidamide treatment (Fig. 6A – 6C). The GSEA plot Fig. 6A shows that chidamide treatment of Jurkat and MOLT-4 cells induces downregulation of proliferation genes which are also known to be downregulated by the HDAC inhibitor SAHA, suggesting that some HDAC downstream genes are indeed targeted by chidamide treatment in these cells and that chidamide target genes at least partially overlap genes targeted by other HDAC inhibitors. Additionally, GSEA plots with genesets corresponding to genes known to be downregulated upon the knock down of HDAC1 or HDAC2 in U2OS cells (Fig. 6B and 6C, respectively) are significantly enriched in our cells upon chidamide treatment, suggesting that chidamide could also have specific effects on these two HDACs' direct or indirect downstream genes.

Additionally, this analysis also pointed to a strong anti-proliferative effect of the chidamide treatment (Fig. 6D), in addition to significant anti-MYC and anti-NOTCH1 effects (Fig. 6E–6I)).

These transcriptomic analyses nicely support the conclusions of all our molecular investigations reported here demonstrating that chidamide is acting at multiple levels, on cell proliferation as well as at specific levels with anti-MYC and anti-NOTCH1 effects.

The presence of a gene expression profile similar to that induced in chidamide-treated cells is associated with longer survival and favorable prognosis in T-ALL patients

To investigate the potential benefit of the molecular response after chidamide treatment for T-ALL patients, we characterized the gene expression profile of the cell lines after chidamide treatment, meaning that we established lists of chidamide responsive genes, either upregulated or downregulated in chidamide-treated cells, as described above. The expression of the genes of these two lists was then measured in each of the leukemic cell samples of 130 newly diagnosed T-ALL patients using the RNAseq expression data. The aim was to identify patients whose leukemic cells presented a gene expression pattern naturally similar to that of chidamide-treated cell lines, which we named here "chidamide-induced profile," and to test the potential association between the presence of this "chidamide-induced profile" in T-ALL patients and their survival probability.

This analysis enabled the identification of 6 patients with a gene expression profile highly similar to the gene expression signature obtained after chidamide treatment in our two cell lines. All these 6 patients carried *NOTCH1* mutations (Table S2).

Clinical data, including survival data, were available for the 130 patients, encompassing these 6 patients [11]. A comparison of the survival probabilities between these 6 patients with a "chidamide-induced profile" and all the other patients demonstrated that all 6 patients with a "chidamide-like" profile have significantly longer survival probability compared to that of the other T-ALL patients (Fig. S4A). This observation strongly suggests that chidamide treatment of T-ALL patient could induce a gene expression profile that is associated with good prognosis in T-ALL patients. A GSEA was performed to identify specific genesets most enriched or depleted in this chidamide-like transcriptomic profile. As expected, this analysis enabled us to confirm the high similarities between the transcriptomic profiles of these patients and of chidamide-treated cells (not shown). Interestingly, the genesets of NOTCH1 co-expressed genes and anti-regulated genes were respectively significantly depleted and enriched in the expression profile of these 6 patients compared to the other TALL. This observation suggests that, in the context of T-ALL, chidamide treatment could be associated with the downregulation of NOTCH1gene expression signature (Fig. S4B and S4C).

Chidamide combined with chemotherapy regimens decreases MRD in T-ALL patients with NOTCH1 mutation

In parallel with these investigations, we set up a clinical trial involving patients newly diagnosed with T-ALL or suffering from relapse by histology or cytology after 2017. Some patients carrying *NOTCH1* mutation received chidamide combined with Hyper-CVAD-A, alternating with chidamide combined with Hyper-CVAD-B monthly.

In the initial results of this pilot clinical trial, we found that in T-ALL patients with *NOTCH1* mutations, no matter newly diagnosed patients or relapsed patients, the combination of chidamide on the basis of chemotherapy regimens can significantly reduce MRD. Patient 2 was a

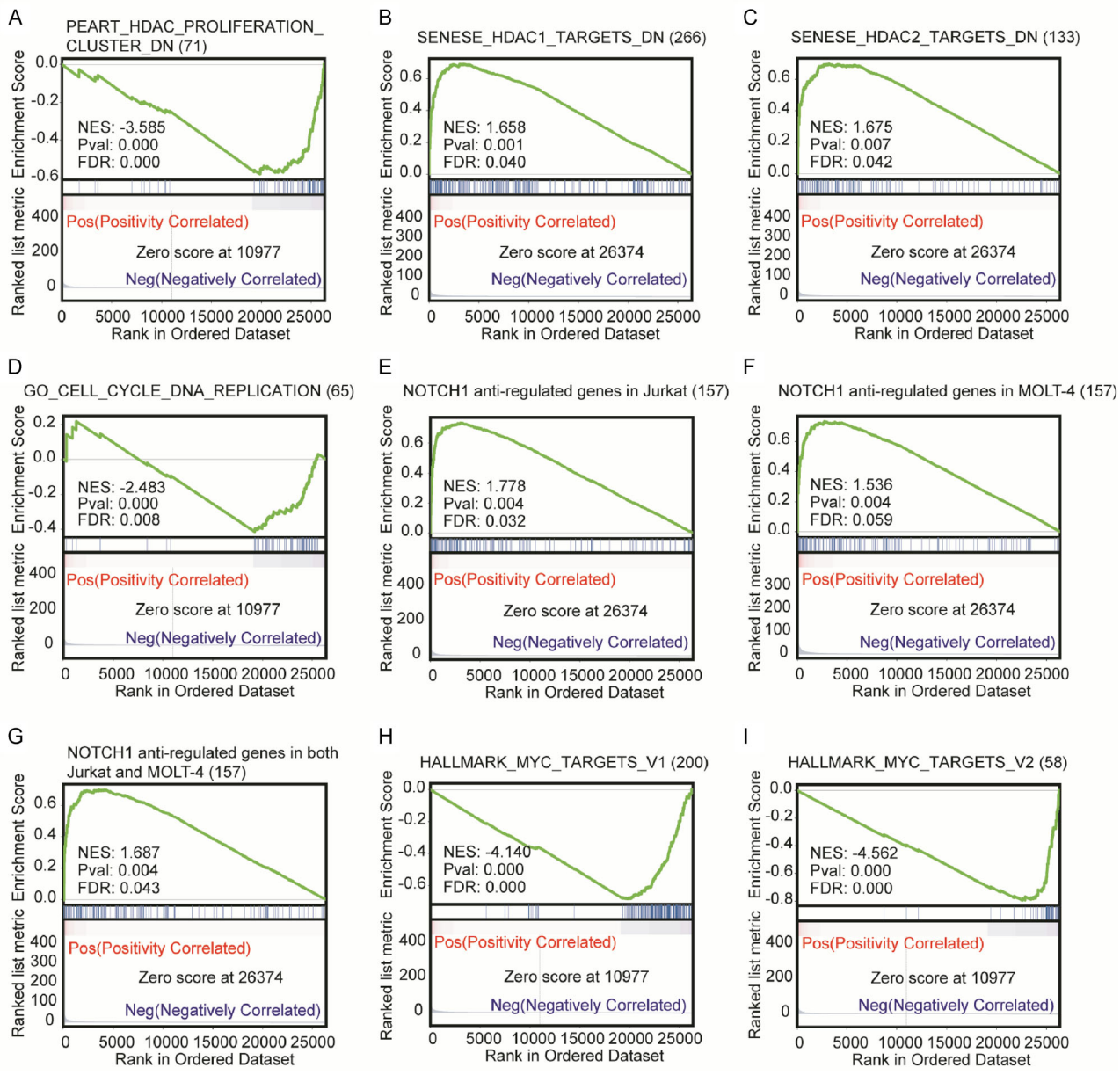

Fig. 6 GSEA analysis in Jurkat and MOLT-4 cell lines. (A–C) Chidamide has a "HDAC inhibitor-like" effect on gene expression in Jurkat and MOLT-4 cell lines. Proliferation HDAC dependent genes are downregulated by chidamide (A), whereas genes normally downregulated by HDAC1 or HDAC2 are overexpressed in chidamide-treated cells (B and C). (D) Chidamide causes significant downregulation of genes involved in cell cycle. (E–G) Chidamide treatment causes a significant upregulation of a set of genes anti-regulated with NOTCH1 (genes whose expressions are anti-correlated with NOTCH1 expression in ALL samples, with Pearson and Spearman coefficients < -0.6) in the two cell lines Jurkat (E) and MOLT-4 (F) respectively, or considering both cell lines (G). (H and I) MYC target genes are significantly downregulated in chidamide-treated Jurkat and MOLT-4 cells as exemplified here with these two genesets from the "hallmark" category of MsigDB.

relapsed patient with *NOTCH1* mutations, and, although MRD was fluctuating, this patient remained in a disease-free state (Fig. 7A). Patients 3 and 4 were newly diagnosed patients carrying *NOTCH1* mutations. In patient 3, MRD was below 0.01% after chemotherapy combined with chidamide (Fig. 7B and 7C). Patient 9 was a relapsed patient whose MRD turned negative after chemotherapy combined with chidamide and successfully completed allogeneic bone marrow transplantation during treatment (Fig. S6D). Patient 8 was a newly diagnosed T-ALL without *NOTCH1* mutations, who showed no reduction in MRD after taking chidamide combined with chemotherapy regimens (Fig. S6E) and who died of central nervous system leukemia (CNSL) soon after diagnosis. We recorded the most serious adverse drug-related events that occurred in the above three patients during the

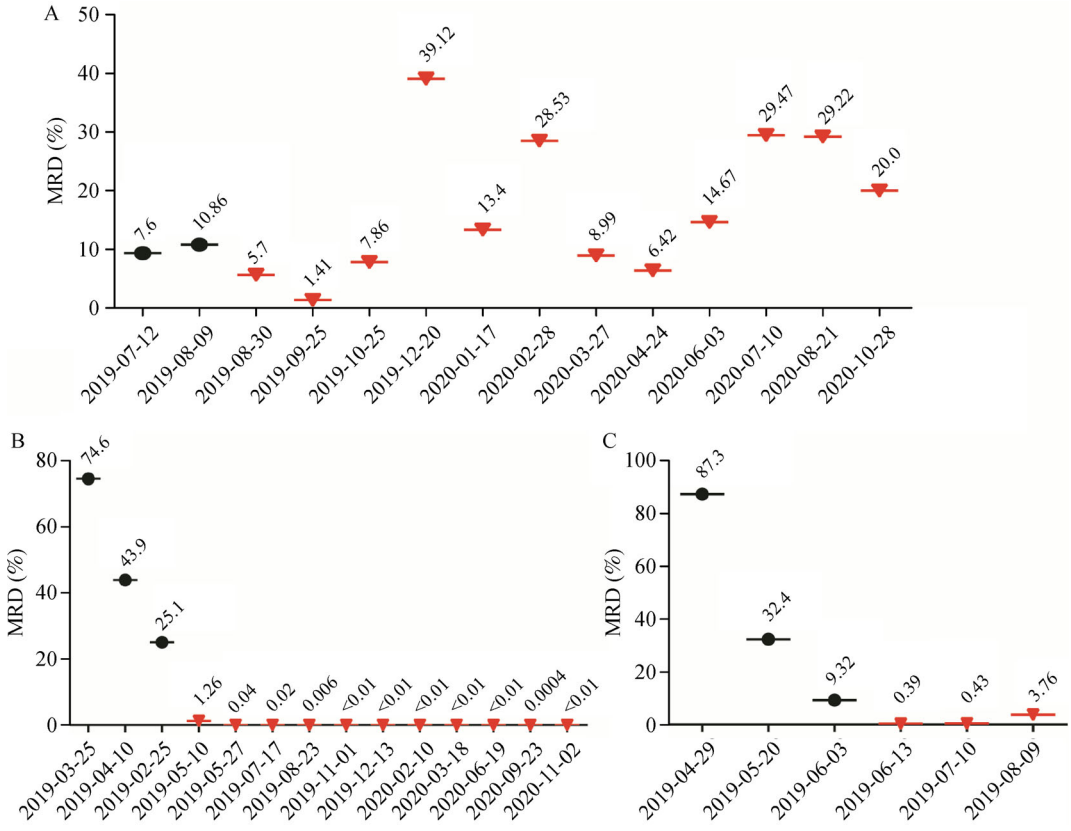

Fig. 7 Chidamide combined with chemotherapy regimens decreases MRD in patient primary cells with NOTCH1 mutation. The black icons mean that the patient only received chemotherapy regimens (Hyper-CVAD-A, alternating with Hyper-CVAD-B monthly). The red icons mean that the patient received chidamide combined with Hyper-CVAD-A, alternating with chidamide combined with Hyper-CVAD-B monthly. (A) Patient 2 was a relapsed patient with NOTCH1 mutations, this patient remained in a disease-free state after taking chidamide combined with chemotherapy regimens. (B) Patient 3, a newly diagnosed T-ALL carrying NOTCH1 mutations, showed a decrease of MRD below 0.01% after chidamide combined with chemotherapy regimens. (C) Patient 4 was also a newly diagnosed patient carrying NOTCH1 mutations, and showed a decrease of MRD after chidamide combined with chemotherapy regimens.

medication (Tables S3 – S7). The most common adverse drug event was thrombocytopenia, which can be relieved by temporarily suspending chidamide.

The results of this clinical trial complement our molecular investigations and strongly support our conclusions on the interest of chidamide as an effective strategy to treat T-ALL patients including those bearing *NOTCH1* mutations.

Discussion

The NOTCH signaling pathway plays an important role in the occurrence and development of T-ALL disease [55,56]. At present, there is no safe and effective NOTCH1 inhibitor in clinical practice [57], so direct inhibition of *NOTCH1* target genes has become an outstanding goal. Among the many target genes of *NOTCH1*, *MYC* has been confirmed to be the central oncogene of T-ALL [21]. The oncogenic activity of NOTCH1 in T-ALL depends on the upregulation of *MYC*, which makes the NOTCH1-MYC axis an attractive therapeutic target for T-ALL treatment. Additionally, MYC also lacks safe and effective inhibitors. Therefore, indirectly targeting MYC to inhibit the NOTCH1-MYC signal axis appears as a key strategy to treat T-ALL patients.

With this respect, encouraging data come from the use of the non-selective HDAC inhibitor panobinostat which significantly downregulated the expression of *NOTCH1* in the PDX model of T-ALL patients with *NOTCH1* mutation. This treatment also reduced tumor burden in the studied mice models and prolonged survival [27].

In line with these data, a recent clinical study reported that the more specific HDAC inhibitor, chidamide combined with chemotherapy could induce higher complete response rate (CRR) and overall response rate (ORR), and better progress-free survival (PFS) in refractory and relapsed T lymphoblastic lymphoma/leukemia, compared with conventional combination chemotherapy [39].

The preliminary results of our clinical trial presented

here support these conclusions and show that the combination of chidamide and chemotherapy could reduce MRD in patients with initial and recurrent refractory T-ALL.

Mechanistically, we observed that the transcriptional level of *NOTCH1* was reduced after treatment with chidamide of one relapsed patient (data not shown), and that the MRD level has remained low until now without tumor-related adverse events.

Our investigations suggest that chidamide is effectively inhibiting the NOTCH1-MYC signaling axis and most interestingly that it induces a gene expression profile in the T-ALL cells that is highly similar to that of patients with favorable prognosis.

We found that chidamide promotes protein degradation through the proteasome pathway by upregulating the ubiquitination levels of NICD1 and MYC. Among the HDAC targets of chidamide, there is HDAC3. It has been reported in the literature that HDAC3 deacetylates the eight lysine residues located within the central part of the NICD1 protein to block the ubiquitination-dependent proteasome degradation pathway and enhance the stability of NICD protein [28]. HDAC3 inhibitors therefore can cause reversible acetylation of NICD1, thereby enhancing its ubiquitination, leading to the degradation of the protein through the proteasome pathway [28]. Chidamide is a selective HDAC inhibitor that can specifically inhibit HDAC1, HDAC2, HDAC3, and HDAC10. Therefore, chidamide treatment may acetylate lysine residues in NICD and MYC proteins by inhibiting HDAC3, which could increase the ubiquitination level of NICD and MYC and promote protein degradation.

This is in line with the results of our study showing that chidamide not only can inhibit *NOTCH1* transcription, but also promotes the ubiquitination and degradation of NICD1 and MYC proteins.

The mechanisms underlying the post-translational regulation of MYC by chidamide remain to be elucidated. Theoretically, chidamide treatment of the cell lines increases the degradation of the intracellular activation fragment (NICD) of NOTCH1 therefore downregulating its target genes. However, chidamide treatment could also counteract this transcriptional downregulation, specifically that of *MYC*. Indeed, NOTCH1 regulates the transcriptional activity of *MYC* through the N-Me (NOTCH1 MYC Enhancer) enhancer element [58,59]. The activity of this enhancer is dependent on BRD4 [60], an epigenetic regulator that binds the H3K27 acetylation mark [61]. We found that chidamide significantly upregulates the level of H3K27 acetylation in Jurkat and MOLT-4 (Fig. S5), which may lead to *MYC* transcriptional activation. Additionally, in the T-ALL studied by King and colleagues, MYC, NOTCH1, and BRD4 extensively co-localize, especially at enhancers [61,62].

Therefore, chidamide treatment increases the degradation of NICD1, which should lead to the inhibition of *MYC* transcription, but could also counteract this effect by enhancing *MYC* transcription. In support of this observation, previous research work has shown that the non-selective HDAC inhibitor SAHA (sulfonylanilide hydroxylamine, also known as vorinostat) does not affect the expression of some *NOTCH1* target genes, including *MYC* [28]. In addition, it has been reported that inhibiting HDAC can promote the expression of some other *NOTCH1* target genes [63].

In conclusion, our experimental results indicate that chidamide shows significant anti-proliferation and more specifically anti-NOTCH1 effects in both cell lines and primary cells of T-ALL patients. By analyzing the expression profile characterizing the response of the cell lines to chidamide treatment, we further confirmed that the antitumor effect of chidamide was due to both the general anti-oncogenic effects of HDAC inhibitors as well as to the anti-NOTCH1 effect. Moreover, the preliminary results of our clinical trials showed that the MRD of the subjects decreased after chidamide treatment and the expression of *NOTCH1* mutant transcripts also decreased in some patients. Our results support that the effectiveness and safety of chidamide treatment in T-ALL patients with *NOTCH1* mutation provide a new therapeutic regimen for T-ALL patients with *NOTCH1* mutation.

Acknowledgements

This study was funded by the Shanghai Science and Technology Committee (No. 21430711800), National Natural Science Foundation of China (Nos. 81670147, 81570178, and Antrag M-0377), Gaofeng Clinical Medicine Grant Support of Shanghai Municipal Education (No. 20172002), Shanghai Municipal Education Commission-Major Project for Scientific Research and Innovation Plan of Natural Science (No. 2021-01-07-00-02-E00091). SK laboratory is supported by "Fondation ARC" grant (PGA1RF20190208471) and the ANR EpiSperm 4 program. Additional supports were from the "Université Grenoble Alpes" ANR-15-IDEX-02 LIFE and SYMER programs, as well as the INSERM/ITMO/Aviesan MIC 2021 program (project ECTOCAN).

Compliance with ethics guidelines

Mengping Xi, Shanshan Guo, Caicike Bayin, Lijun peng, Florent Chuffart, Ekaterina Bourova-Flin, Sophie Rousseaux, Saadi Khochbin, Jian-Qing Mi, and Jin Wang declare that they have no conflict of interest. All procedures performed in studies involving human samples were approved by the ethics committee at Ruijin Hospital, Shanghai Jiao Tong University School of Medicine and Shanghai Blood Center, and in accordance with the principles of the 1964 *Declaration of Helsinki* and its later amendments or comparable ethical standards. All patients gave written informed consent prior to bone marrow sample collection for the use of biomaterials and clinical data for scientific purposes.

Electronic Supplementary Material Supplementary material is available in the online version of this article at https://doi.org/10.1007/s11684-021-0877-y and is accessible for authorized users.

References

1. Alvarnas JC, Brown PA, Aoun P, Ballen KK, Barta SK, Borate U, Boyer MW, Burke PW, Cassaday R, Castro JE, Coccia PF, Coutre SE, Damon LE, DeAngelo DJ, Douer D, Frankfurt O, Greer JP, Johnson RA, Kantarjian HM, Klisovic RB, Kupfer G, Litzow M, Liu A, Rao AV, Shah B, Uy GL, Wang ES, Zelenetz AD, Gregory K, Smith C. Acute Lymphoblastic Leukemia, Version 2.2015. J Natl Compr Canc Netw 2015; 13(10): 1240–1279
2. Hunger SP, Mullighan CG. Acute lymphoblastic leukemia in children. N Engl J Med 2015; 373(16): 1541–1552
3. Aref S, El Agdar M, Salama O, Zeid TA, Sabry M. Significance of NOTCH1 mutations détections in T-acute lymphoblastic leukemia patients. Cancer Biomark 2020; 27(2): 157–162
4. Guru Murthy GS, Pondaiah SK, Abedin S, Atallah E. Incidence and survival of T-cell acute lymphoblastic leukemia in the United States. Leuk Lymphoma 2019; 60(5): 1171–1178
5. Aldoss I, Stein AS. Advances in adult acute lymphoblastic leukemia therapy. Leuk Lymphoma 2018; 59(5): 1033–1050
6. DeAngelo DJ, Yu D, Johnson JL, Coutre SE, Stone RM, Stopeck AT, Gockerman JP, Mitchell BS, Appelbaum FR, Larson RA. Nelarabine induces complete remissions in adults with relapsed or refractory T-lineage acute lymphoblastic leukemia or lymphoblastic lymphoma: Cancer and Leukemia Group B study 19801. Blood 2007; 109(12): 5136–5142
7. Caracciolo D, Riillo C, Ballerini A, Gaipa G, Lhermitte L, Rossi M, Botta C, Duroyon E, Grillone K, Gallo Cantafio ME, Buracchi C, Alampi G, Gulino A, Belmonte B, Conforti F, Golino G, Juli G, Altomare E, Polerà N, Scionti F, Arbitrio M, Iannone M, Martino M, Correale P, Talarico G, Ghelli Luserna di Rorà A, Ferrari A, Concolino D, Sestito S, Pensabene L, Giordano A, Hildinger M, Di Martino MT, Martinelli G, Tripodo C, Asnafi V, Biondi A, Tagliaferri P, Tassone P. Therapeutic afucosylated monoclonal antibody and bispecific T-cell engagers for T-cell acute lymphoblastic leukemia. J Immunother Cancer 2021; 9(2): e002026
8. You MJ, Medeiros LJ, Hsi ED. T-lymphoblastic leukemia/lymphoma. Am J Clin Pathol 2015; 144(3): 411–422
9. Girardi T, Vicente C, Cools J, De Keersmaecker K. The genetics and molecular biology of T-ALL. Blood 2017; 129(9): 1113–1123
10. Liu Y, Easton J, Shao Y, Maciaszek J, Wang Z, Wilkinson MR, McCastlain K, Edmonson M, Pounds SB, Shi L, Zhou X, Ma X, Sioson E, Li Y, Rusch M, Gupta P, Pei D, Cheng C, Smith MA, Auvil JG, Gerhard DS, Relling MV, Winick NJ, Carroll AJ, Heerema NA, Raetz E, Devidas M, Willman CL, Harvey RC, Carroll WL, Dunsmore KP, Winter SS, Wood BL, Sorrentino BP, Downing JR, Loh ML, Hunger SP, Zhang J, Mullighan CG. The genomic landscape of pediatric and young adult T-lineage acute lymphoblastic leukemia. Nat Genet 2017; 49(8): 1211–1218
11. Chen B, Jiang L, Zhong ML, Li JF, Li BS, Peng LJ, Dai YT, Cui BW, Yan TQ, Zhang WN, Weng XQ, Xie YY, Lu J, Ren RB, Chen SN, Hu JD, Wu DP, Chen Z, Tang JY, Huang JY, Mi JQ, Chen SJ. Identification of fusion genes and characterization of transcriptome features in T-cell acute lymphoblastic leukemia. Proc Natl Acad Sci USA 2018; 115(2): 373–378
12. Yuan L, Lu L, Yang Y, Sun H, Chen X, Huang Y, Wang X, Zou L, Bao L. Genetic mutational profiling analysis of T cell acute lymphoblastic leukemia reveal mutant FBXW7 as a prognostic indicator for inferior survival. Ann Hematol 2015; 94(11): 1817–1828
13. Yeh CH, Bellon M, Pancewicz-Wojtkiewicz J, Nicot C. Oncogenic mutations in the FBXW7 gene of adult T-cell leukemia patients. Proc Natl Acad Sci USA 2016; 113(24): 6731–6736
14. Hefazi M, Litzow MR. Recent advances in the biology and treatment of T cell acute lymphoblastic leukemia. Curr Hematol Malig Rep 2018; 13(4): 265–274
15. McCarter AC, Wang Q, Chiang M. Notch in leukemia. Adv Exp Med Biol 2018; 1066: 355–394
16. Takebe N, Nguyen D, Yang SX. Targeting notch signaling pathway in cancer: clinical development advances and challenges. Pharmacol Ther 2014; 141(2): 140–149
17. Kaushik B, Pal D, Saha S. Gamma secretase inhibitor: therapeutic target via NOTCH signaling in T cell acute lymphoblastic leukemia. Curr Drug Targets 2021; [Epub ahead of print] doi: 10.2174/1389450122666210203192752
18. Palomero T, Lim WK, Odom DT, Sulis ML, Real PJ, Margolin A, Barnes KC, O'Neil J, Neuberg D, Weng AP, Aster JC, Sigaux F, Soulier J, Look AT, Young RA, Califano A, Ferrando AA. NOTCH1 directly regulates c-MYC and activates a feed-forward-loop transcriptional network promoting leukemic cell growth. Proc Natl Acad Sci USA 2006; 103(48): 18261–18266
19. Margolin AA, Palomero T, Sumazin P, Califano A, Ferrando AA, Stolovitzky G. ChIP-on-chip significance analysis reveals large-scale binding and regulation by human transcription factor oncogenes. Proc Natl Acad Sci USA 2009; 106(1): 244–249
20. Jiang J, Wang J, Yue M, Cai X, Wang T, Wu C, Su H, Wang Y, Han M, Zhang Y, Zhu X, Jiang P, Li P, Sun Y, Xiao W, Feng H, Qing G, Liu H. Direct phosphorylation and stabilization of MYC by Aurora B kinase promote T-cell leukemogenesis. Cancer Cell 2020; 37(2): 200–215.e5
21. Sanchez-Martin M, Ferrando A. The NOTCH1-MYC highway toward T-cell acute lymphoblastic leukemia. Blood 2017; 129(9): 1124–1133
22. Chiang MY, Wang Q, Gormley AC, Stein SJ, Xu L, Shestova O, Aster JC, Pear WS. High selective pressure for Notch1 mutations that induce Myc in T-cell acute lymphoblastic leukemia. Blood 2016; 128(18): 2229–2240
23. Loosveld M, Castellano R, Gon S, Goubard A, Crouzet T, Pouyet L, Prebet T, Vey N, Nadel B, Collette Y, Payet-Bornet D. Therapeutic targeting of c-Myc in T-cell acute lymphoblastic leukemia, T-ALL. Oncotarget 2014; 5(10): 3168–3172
24. McKeown MR, Bradner JE. Therapeutic strategies to inhibit MYC. Cold Spring Harb Perspect Med 2014; 4(10): a014266
25. Beyer M, Romanski A, Mustafa AM, Pons M, Büchler I, Vogel A, Pautz A, Sellmer A, Schneider G, Bug G, Krämer OH. HDAC3 activity is essential for human leukemic cell growth and the expression of β-catenin, MYC, and WT1. Cancers (Basel) 2019; 11(10): 1436
26. Sun K, Atoyan R, Borek MA, Dellarocca S, Samson ME, Ma AW, Xu GX, Patterson T, Tuck DP, Viner JL, Fattaey A, Wang J. Dual

HDAC and PI3K inhibitor CUDC-907 downregulates MYC and suppresses growth of MYC-dependent cancers. Mol Cancer Ther 2017; 16(2): 285–299

27. Waibel M, Vervoort SJ, Kong IY, Heinzel S, Ramsbottom KM, Martin BP, Hawkins ED, Johnstone RW. Epigenetic targeting of Notch1-driven transcription using the HDACi panobinostat is a potential therapy against T-cell acute lymphoblastic leukemia. Leukemia 2018; 32(1): 237–241
28. Ferrante F, Giaimo BD, Bartkuhn M, Zimmermann T, Close V, Mertens D, Nist A, Stiewe T, Meier-Soelch J, Kracht M, Just S, Klöble P, Oswald F, Borggrefe T. HDAC3 functions as a positive regulator in Notch signal transduction. Nucleic Acids Res 2020; 48(7): 3496–3512
29. Reynoird N, Schwartz BE, Delvecchio M, Sadoul K, Meyers D, Mukherjee C, Caron C, Kimura H, Rousseaux S, Cole PA, Panne D, French CA, Khochbin S. Oncogenesis by sequestration of CBP/p300 in transcriptionally inactive hyperacetylated chromatin domains. EMBO J 2010; 29(17): 2943–2952
30. Delmore JE, Issa GC, Lemieux ME, Rahl PB, Shi J, Jacobs HM, Kastritis E, Gilpatrick T, Paranal RM, Qi J, Chesi M, Schinzel AC, McKeown MR, Heffernan TP, Vakoc CR, Bergsagel PL, Ghobrial IM, Richardson PG, Young RA, Hahn WC, Anderson KC, Kung AL, Bradner JE, Mitsiades CS. BET bromodomain inhibition as a therapeutic strategy to target c-Myc. Cell 2011; 146(6): 904–917
31. Suresh PS, Devaraj VC, Srinivas NR, Mullangi R. Review of bioanalytical assays for the quantitation of various HDAC inhibitors such as vorinostat, belinostat, panobinostat, romidepsin and chidamine. Biomed Chromatogr 2017; 31(1): e3807
32. Liu Z, Ding K, Li L, Liu H, Wang Y, Liu C, Fu R. A novel histone deacetylase inhibitor chidamide induces G0/G1 arrest and apoptosis in myelodysplastic syndromes. Biomed Pharmacother 2016; 83: 1032–1037
33. Zhao S, Guo J, Zhao Y, Fei C, Zheng Q, Li X, Chang C. Chidamide, a novel histone deacetylase inhibitor, inhibits the viability of MDS and AML cells by suppressing JAK2/STAT3 signaling. Am J Transl Res 2016; 8(7): 3169–3178
34. Jiang T, Wang F, Hu L, Cheng X, Zheng Y, Liu T, Jia Y. Chidamide and decitabine can synergistically induce apoptosis of Hodgkin lymphoma cells by up-regulating the expression of PU.1 and KLF4. Oncotarget 2017; 8(44): 77586–77594
35. He J, Chen Q, Gu H, Chen J, Zhang E, Guo X, Huang X, Yan H, He D, Yang Y, Zhao Y, Wang G, He H, Yi Q, Cai Z. Therapeutic effects of the novel subtype-selective histone deacetylase inhibitor chidamide on myeloma-associated bone disease. Haematologica 2018; 103(8): 1369–1379
36. Zhou J, Zhang C, Sui X, Cao S, Tang F, Sun S, Wang S, Chen B. Histone deacetylase inhibitor chidamide induces growth inhibition and apoptosis in NK/T lymphoma cells through ATM-Chk2-p53-p21 signalling pathway. Invest New Drugs 2018; 36(4): 571–580
37. Shi Y, Jia B, Xu W, Li W, Liu T, Liu P, Zhao W, Zhang H, Sun X, Yang H, Zhang X, Jin J, Jin Z, Li Z, Qiu L, Dong M, Huang X, Luo Y, Wang X, Wang X, Wu J, Xu J, Yi P, Zhou J, He H, Liu L, Shen J, Tang X, Wang J, Yang J, Zeng Q, Zhang Z, Cai Z, Chen X, Ding K, Hou M, Huang H, Li X, Liang R, Liu Q, Song Y, Su H, Gao Y, Liu L, Luo J, Su L, Sun Z, Tan H, Wang H, Wang J, Wang S, Zhang H, Zhang X, Zhou D, Bai O, Wu G, Zhang L, Zhang Y. Chidamide in relapsed or refractory peripheral T cell lymphoma: a multicenter real-world study in China. J Hematol Oncol 2017; 10(1): 69
38. Lu X, Ning Z, Li Z, Cao H, Wang X. Development of chidamide for peripheral T-cell lymphoma, the first orphan drug approved in China. Intractable Rare Dis Res 2016; 5(3): 185–191
39. Guan W, Jing Y, Dou L, Wang M, Xiao Y, Yu L. Chidamide in combination with chemotherapy in refractory and relapsed T lymphoblastic lymphoma/leukemia. Leuk Lymphoma 2020; 61(4): 855–861
40. Weng XQ, Shen Y, Sheng Y, Chen B, Wang JH, Li JM, Mi JQ, Chen QS, Zhu YM, Jiang CL, Yan H, Zhang XX, Huang T, Zhu Z, Chen Z, Chen SJ. Prognostic significance of monitoring leukemia-associated immunophenotypes by eight-color flow cytometry in adult B-acute lymphoblastic leukemia. Blood Cancer J 2013; 3(8): e133
41. Zhu YM, Zhao WL, Fu JF, Shi JY, Pan Q, Hu J, Gao XD, Chen B, Li JM, Xiong SM, Gu LJ, Tang JY, Liang H, Jiang H, Xue YQ, Shen ZX, Chen Z, Chen SJ. NOTCH1 mutations in T-cell acute lymphoblastic leukemia: prognostic significance and implication in multifactorial leukemogenesis. Clin Cancer Res 2006; 12(10): 3043–3049
42. Dobin A, Davis CA, Schlesinger F, Drenkow J, Zaleski C, Jha S, Batut P, Chaisson M, Gingeras TR. STAR: ultrafast universal RNA-seq aligner. Bioinformatics 2013; 29(1): 15–21
43. Anders S, Pyl PT, Huber W. HTSeq—a Python framework to work with high-throughput sequencing data. Bioinformatics 2015; 31(2): 166–169
44. Varet H, Brillet-Guéguen L, Coppée JY, Dillies MA. SARTools: a DESeq2- and EdgeR-based R pipeline for comprehensive differential analysis of RNA-Seq data. PLoS One 2016; 11(6): e0157022
45. Xu JJ, Yao FR, Jiang M, Zhang YT, Guo F. High-resolution melting analysis for rapid and sensitive NOTCH1 screening in chronic lymphocytic leukemia. Int J Mol Med 2017; 39(2): 415–422
46. Squiban B, Ahmed ST, Frazer JK. Creation of a human T-ALL cell line online database. Leuk Lymphoma 2017; 58(11): 2728–2730
47. Sulis ML, Williams O, Palomero T, Tosello V, Pallikuppam S, Real PJ, Barnes K, Zuurbier L, Meijerink JP, Ferrando AA. NOTCH1 extracellular juxtamembrane expansion mutations in T-ALL. Blood 2008; 112(3): 733–740
48. Horvat L, Antica M, Matulić M. Effect of Notch and PARP pathways' inhibition in leukemic cells. Cells 2018; 7(6): 58
49. Gui CY, Ngo L, Xu WS, Richon VM, Marks PA. Histone deacetylase (HDAC) inhibitor activation of p21WAF1 involves changes in promoter-associated proteins, including HDAC1. Proc Natl Acad Sci USA 2004; 101(5): 1241–1246
50. Stengel KR, Hiebert SW. Class I HDACs affect DNA replication, repair, and chromatin structure: implications for cancer therapy. Antioxid Redox Signal 2015; 23(1): 51–65
51. Boulaire J, Fotedar A, Fotedar R. The functions of the cdk-cyclin kinase inhibitor p21WAF1. Pathol Biol (Paris) 2000; 48(3): 190–202
52. Radtke F, Wilson A, Mancini SJ, MacDonald HR. Notch regulation of lymphocyte development and function. Nat Immunol 2004; 5(3): 247–253
53. Osborne BA, Minter LM. Notch signalling during peripheral T-cell activation and differentiation. Nat Rev Immunol 2007; 7(1): 64–75
54. Yu VW, Saez B, Cook C, Lotinun S, Pardo-Saganta A, Wang YH, Lymperi S, Ferraro F, Raaijmakers MH, Wu JY, Zhou L, Rajagopal

J, Kronenberg HM, Baron R, Scadden DT. Specific bone cells produce DLL4 to generate thymus-seeding progenitors from bone marrow. J Exp Med 2015; 212(5): 759–774

55. Malard F, Mohty M. Acute lymphoblastic leukaemia. Lancet 2020; 395(10230): 1146–1162
56. De Bie J, Demeyer S, Alberti-Servera L, Geerdens E, Segers H, Broux M, De Keersmaecker K, Michaux L, Vandenberghe P, Voet T, Boeckx N, Uyttebroeck A, Cools J. Single-cell sequencing reveals the origin and the order of mutation acquisition in T-cell acute lymphoblastic leukemia. Leukemia 2018; 32(6): 1358–1369
57. Roti G, Qi J, Kitara S, Sanchez-Martin M, Saur Conway A, Varca AC, Su A, Wu L, Kung AL, Ferrando AA, Bradner JE, Stegmaier K. Leukemia-specific delivery of mutant NOTCH1 targeted therapy. J Exp Med 2018; 215(1): 197–216
58. Herranz D, Ambesi-Impiombato A, Palomero T, Schnell SA, Belver L, Wendorff AA, Xu L, Castillo-Martin M, Llobet-Navás D, Cordon-Cardo C, Clappier E, Soulier J, Ferrando AAA. A NOTCH1-driven MYC enhancer promotes T cell development, transformation and acute lymphoblastic leukemia. Nat Med 2014; 20(10): 1130–1137
59. Herranz D, Ferrando AA. An oncogenic enhancer enemy (N-Me) in T-ALL. Cell Cycle 2015; 14(2): 167–168
60. Sengupta D, Kannan A, Kern M, Moreno MA, Vural E, Stack B Jr, Suen JY, Tackett AJ, Gao L. Disruption of BRD4 at H3K27Ac-enriched enhancer region correlates with decreased c-Myc expression in Merkel cell carcinoma. Epigenetics 2015; 10(6): 460–466
61. Lovén J, Hoke HA, Lin CY, Lau A, Orlando DA, Vakoc CR, Bradner JE, Lee TI, Young RA. Selective inhibition of tumor oncogenes by disruption of super-enhancers. Cell 2013; 153(2): 320–334
62. Levens D, Aplan PD. Notching up MYC gives a LIC. Cell Stem Cell 2013; 13(1): 8–9
63. Cheng CW, Biton M, Haber AL, Gunduz N, Eng G, Gaynor LT, Tripathi S, Calibasi-Kocal G, Rickelt S, Butty VL, Moreno-Serrano M, Iqbal AM, Bauer-Rowe KE, Imada S, Ulutas MS, Mylonas C, Whary MT, Levine SS, Basbinar Y, Hynes RO, Mino-Kenudson M, Deshpande V, Boyer LA, Fox JG, Terranova C, Rai K, Piwnica-Worms H, Mihaylova MM, Regev A, Yilmaz OH. Ketone body signaling mediates intestinal stem cell homeostasis and adaptation to diet. Cell 2019; 178(5): 1115–1131.e15